

Elastic and Inelastic Scattering of ^{14}C by ^{14}C

D. Konnerth, K. G. Bernhardt, K. A. Eberhard, R. Singh,^(a)
 A. Strzalkowski,^(b) W. Trautmann, and W. Trombik
Sektion Physik, Universität München, D-8046 Garching, West Germany
 (Received 14 July 1980)

Elastic scattering cross sections for $^{14}\text{C} + ^{14}\text{C}$ have been measured at 70° , 80° , and 90° (c.m.) in the energy range between 6 and 35 MeV (c.m.). Strongly pronounced, rather regular, gross structure is observed which, at 90° , peaks at 15.5, 19.5, 24, and 28 MeV. The angular distributions suggest a dominance of $l = 12, 14, 16, \text{ and } 18$, respectively, at these energies. Intermediate structure is observed in the single and mutual 3^- , 6.73-MeV inelastic channels above 20 MeV (c.m.).

PACS numbers: 25.70.Hi

The radioactive ^{14}C nucleus is characterized by the closed $p_{1/2}$ neutron shell (of ^{16}O) and the closed $p_{3/2}$ proton subshell (of ^{12}C). With a gap of more than 6 MeV between its ground and first excited states it resembles the doubly closed-shell nucleus ^{16}O . The strikingly large and regular gross structure seen in $^{16}\text{O} + ^{16}\text{O}$ elastic scattering at center of mass energies above 15 MeV has been interpreted as resulting from an extended transparency for surface partial waves.¹ On this basis, a similar behavior is expected for $^{14}\text{C} + ^{14}\text{C}$. On the other hand, the scattering behavior might also be tied to an α -substructure of the colliding nuclei and hence, $^{14}\text{C} + ^{14}\text{C}$ would be different from $^{16}\text{O} + ^{16}\text{O}$, since no substantial α -substructures are expected to exist in ^{14}C . The experimental study of $^{14}\text{C} + ^{14}\text{C}$ scattering is complicated through the use of both a radioactive beam and a radioactive target. These difficulties were overcome in our laboratory by the development of a ^{14}C beam from a sputter source by Kutschera and co-workers² and by preparing thin, self-supporting ^{14}C targets by thermal cracking of $^{14}\text{CH}_3\text{-I}$ by Maier.³ The beam intensity on target was typically about 5 particle \cdot nA. The ^{14}C target contained about 20% ^{12}C . The total target thickness of $96 \pm 17 \mu\text{g}/\text{cm}^2$ was determined from Coulomb scattering at 6 MeV (c.m.) and, independently, from measuring the energy loss of 5.5 MeV α particles passing through the target.

In this Letter, for the first time, experimental results are reported for $^{14}\text{C} + ^{14}\text{C}$ collisions in the energy range 6 MeV to 35 MeV (c.m.).

The various final channels of the $^{14}\text{C} + ^{14}\text{C}$ and $^{14}\text{C} + ^{12}\text{C}$ reactions were unambiguously resolved with use of the technique of kinematical coincidences. Five rectangular Si surface-barrier detectors⁴ (2.5 mm \times 19 mm active area) were used in coincidence with a 46 mm \times 5 mm position-sensitive Si surface-barrier detector which subtend-

ed an angular range of about 20° (lab). The angular resolution was 0.88° (lab) and the experimental energy resolution in the rectangular detectors was determined primarily by kinematical broadening (0.5 MeV at $E_{\text{lab}} = 30$ MeV and 1.0 MeV at $E_{\text{lab}} = 60$ MeV). Substantially better resolutions were obtained in the spectra by adding up the energies in both detectors. Q -value and mass spectra were generated and were used for selection of the various reaction channels.

The excitation function of $^{14}\text{C} + ^{14}\text{C}$ elastic scattering at $\theta_{\text{c.m.}} = 90^\circ$ exhibits a strongly pronounced and rather regular gross structure (Fig. 1). The peak-to-valley ratio exceeds one order of magnitude; the widths are of the order 2–3 MeV (c.m.). It closely resembles the $^{16}\text{O} + ^{16}\text{O}$ data.¹ Similarly pronounced structures are observed at 70° and 80° (c.m.), although they are less regular at 80° .

Because of the striking resemblance to $^{16}\text{O} + ^{16}\text{O}$ scattering we were prompted to use the same optical-model potential as given by Maher *et al.*¹ for $^{16}\text{O} + ^{16}\text{O}$ scattering. Only the imaginary potential had to be modified slightly (larger diffuseness and stronger energy dependence) in order to obtain the qualitative agreement with the data shown in Fig. 1. The slight decrease of the cross section with increasing energy above $E_{\text{c.m.}} = 20$ MeV seems to be better accounted for by the J -dependent potential of Chatwin *et al.*⁵ All parameters used are listed in Table I.

Angular distributions were measured at energies corresponding to peaks in the 90° excitation function (Fig. 2). An attempt to fit these with use of Legendre polynomials clearly singles out $l = 12, 14, 16, \text{ and } 18$, as the dominant partial waves at $E_{\text{c.m.}} = 15.5, 19.5, 24, \text{ and } 28$ MeV, respectively. The systematic deviations of the corresponding $|P_l|^2$ curves from the data indicate, however, that other partial waves contribute also (Fig. 2). Slightly improved fits were

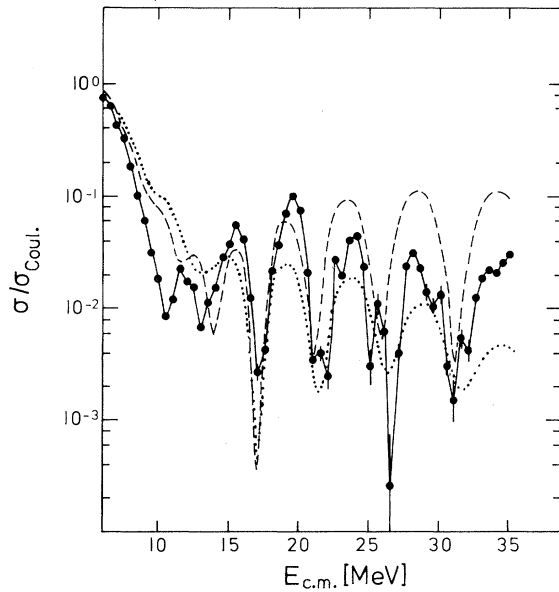


FIG. 1. Elastic scattering of $^{14}\text{C} + ^{14}\text{C}$ at 90° (c.m.) as a function of energy. Statistical errors of the data points are of the order of 10% at the cross section maxima. Optical-model (OM) calculations are shown by the dashed curve (standard OM potential, similar to the $^{16}\text{O} + ^{16}\text{O}$ potential of Ref. 1) and the dotted curve (OM potential with J -dependent absorption). The parameters used are listed in Table I.

obtained by allowing an $(l - 2)$ contribution in the fits with Legendre polynomials.

The optical potentials used are characterized by a considerable surface transparency which, according to the analysis of the measured angular distributions, seems to affect the grazing and—to a lesser extent—the $(l_{gr} - 2)$ partial waves. The surface transparency expresses the lack of other available exit channels besides the elastic channel. This results from angular momentum restrictions: Following Shaw *et al.*⁶ we have calculated the maximum angular momentum compatible with possible direct-reaction channels as a function of energy, using the standard optical model

TABLE I. Optical-model parameters used for the calculations shown in Fig. 1.

	$V(\text{MeV})$	$W_{\text{Vol}}(\text{MeV})$	$r_R(\text{fm})$	$a_R(\text{fm})$	$r_I(\text{fm})$	$a_I(\text{fm})$
Standard	17	$0.8 + 0.5E_{c.m.}$	1.35	0.49	1.27	0.21
J dependent	17	$0.8 + 0.27E_{c.m.}$ ^a	1.35	0.49	1.35	0.49

^aThe same J dependence as for $^{16}\text{O} + ^{16}\text{O}$ (Ref. 6) was used with the only exception of setting $\bar{R} = 7.7$ fm (instead of 6.7 fm) and $\bar{Q} = -7.7$ MeV (instead of -6.7 MeV).

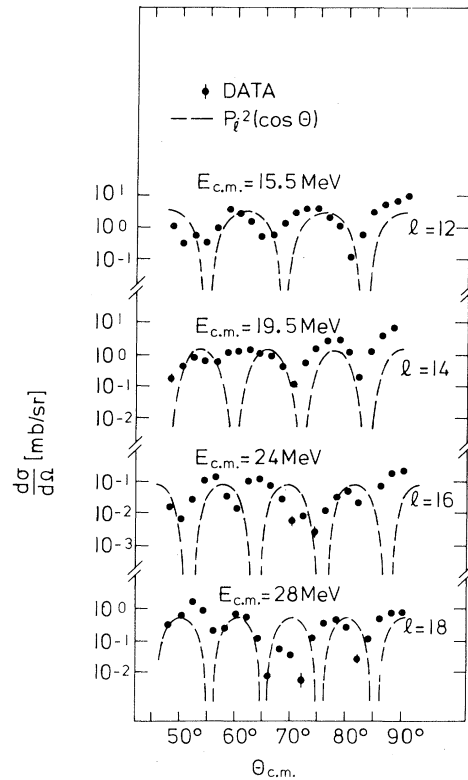


FIG. 2. Angular distributions measured at energies which correspond to the maxima in the 90° (c.m.) excitation function of Fig. 1 along with P_l^2 distributions for the dominant partial waves.

to derive the maximum partial wave; we find that only a few inelastic channels, and only at $E_{c.m.} > 20$ MeV, should couple to the elastic channel whereas most other channels are considerably mismatched.⁷ In this respect $^{14}\text{C} + ^{14}\text{C}$ again resembles $^{16}\text{O} + ^{16}\text{O}$ (cf. Ref. 6). Compound cross sections estimated from Hauser-Feshbach calculations⁸ are found to be orders of magnitude smaller than the observed experimental cross sections, and thus are of no importance here.

The results obtained for single and mutual in-

elastic scattering to the 3^- , 6.73-MeV state of ^{14}C are summarized in Fig. 3. The individual states around 7-MeV excitation in ^{14}C were not resolved in the single inelastic measurement, but the center of the distribution at $Q = -6.74 \pm 0.11$ MeV suggests that the 3^- , 6.73-MeV state is most strongly populated. Mutual inelastic scattering was measured in a separate experiment by using two large size (27 cm \times 33 cm) NaI(Tl) detectors in coincidence, each at 90° with respect to the beam axis and opposite to each other. Here also the 3^- , 6.73-MeV state clearly dominates in the γ -ray spectra. The cross sections for mutual inelastic scattering, between ~ 1 and 10 mb (Fig. 3), are nearly an order of magnitude smaller

than those for $^{12}\text{C} + ^{12}\text{C}$ (Ref. 9). Resonant structures, 0.5 to 1.5 MeV broad, are observed in the inelastic channels (Fig. 3) with no obvious correlation to the gross structures in elastic scattering (Fig. 1).

The following conclusions are drawn from the results observed here:

(1) Any major role of α -substructures concerning elastic and inelastic scattering is ruled out by the great similarity of $^{14}\text{C} + ^{14}\text{C}$ and $^{16}\text{O} + ^{16}\text{O}$ scattering, since α -substructures should be quite different in ^{14}C and ^{16}O .

(2) The pronounced gross structure in $^{14}\text{C} + ^{14}\text{C}$ and $^{16}\text{O} + ^{16}\text{O}$ elastic scattering is a consequence of an extended surface transparency caused by the poor angular momentum matching between the elastic channel and the available reaction channels due to unfavorable reaction Q values and—in the case of inelastic scattering—due to the large energy gap (> 6 MeV) between ground state and first excited states in both ^{14}C and ^{16}O .

(3) No particular resonance mechanism is required to describe the *gross structure*; optical-model potentials with weak absorption for the grazing partial waves well reproduce the observed phenomena.

(4) On the other hand, *resonancelike structures of intermediate width* are present in the inelastic data. The strength of inelastic excitation of these structures, however, is nearly an order of magnitude weaker in $^{14}\text{C} + ^{14}\text{C}$ and in $^{16}\text{O} + ^{16}\text{O}$ (Ref. 10) than observed for $^{12}\text{C} + ^{12}\text{C}$ (Ref. 10) and $^{12}\text{C} + ^{16}\text{O}$ (Ref. 11). The likely reason is that in the case of $^{12}\text{C} + ^{12}\text{C}$ the collective 2^+ , 4.43-MeV state is excited whereas for $^{14}\text{C} + ^{14}\text{C}$ and for $^{16}\text{O} + ^{16}\text{O}$ the excited states are less collective and are at significantly higher excitation energy (3^- , 6.73 MeV for ^{14}C and 3^- , 6.13 MeV for ^{16}O). It is concluded that the strong coupling between elastic and inelastic channels leads to the irregularity in the $^{12}\text{C} + ^{12}\text{C}$ elastic-scattering excitation function.¹² In contrast, for $^{14}\text{C} + ^{14}\text{C}$ and $^{16}\text{O} + ^{16}\text{O}$ the coupling is weak and the elastic-scattering excitation functions show regular gross structure with some coupling effect only seen at higher energies. It should be emphasized that, from surface-transparency arguments only, the different behavior of $^{12}\text{C} + ^{12}\text{C}$ compared to $^{14}\text{C} + ^{14}\text{C}$ and $^{16}\text{O} + ^{16}\text{O}$ cannot be explained since $^{12}\text{C} + ^{12}\text{C}$ is expected to be even more surface transparent than $^{14}\text{C} + ^{14}\text{C}$ and $^{16}\text{O} + ^{16}\text{O}$ from level density calculations.

In summary, it appears that, from the $^{14}\text{C} + ^{14}\text{C}$ results presented here and from a comparison with other systems in this mass region, a rigor-

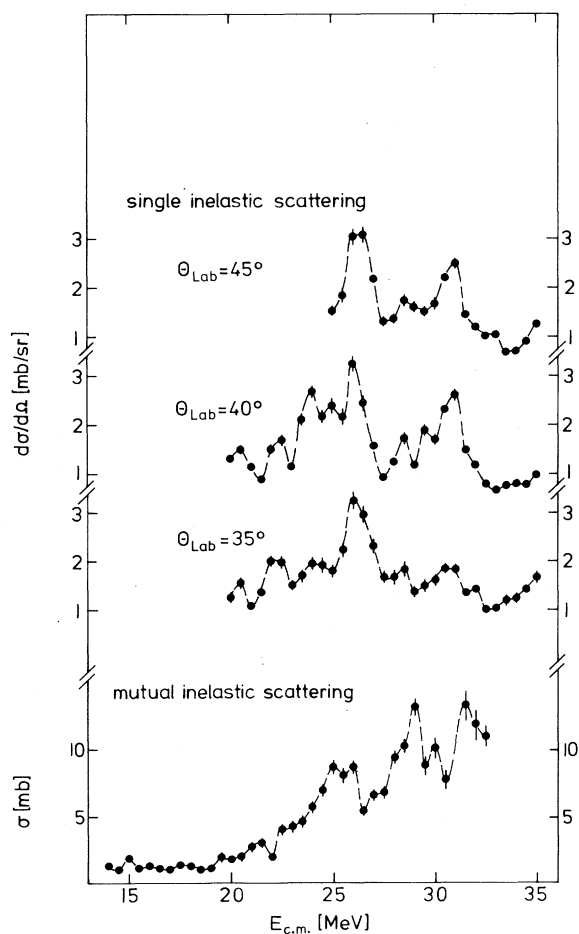


FIG. 3. Excitation functions for inelastic scattering. The three curves on top show cross sections for $^{14}\text{C}(^{14}\text{C}, ^{14}\text{C})^{14}\text{C}^*(3^-, 6.73 \text{ MeV})$ at angles of 45° , 40° , and 35° , respectively. Total cross sections for $^{14}\text{C}[^{14}\text{C}, ^{14}\text{C}^*(3^-, 6.73 \text{ MeV})]^{14}\text{C}^*(3^-, 6.73 \text{ MeV})$, bottom curve, were obtained from a γ - γ coincidence measurement assuming angular isotropy.

ous statement can be made: Elastic-scattering excitation functions for surface transparent systems—such as $^{12}\text{C} + ^{12}\text{C}$, $^{12}\text{C} + ^{16}\text{O}$, $^{14}\text{C} + ^{14}\text{C}$, $^{16}\text{O} + ^{16}\text{O}$, $^{14}\text{C} + ^{16}\text{O}$ (Ref. 13), etc.—are dominated either by (i) pronounced and regular *gross structure*, a few megaelectronvolts broad, if *inelastic coupling is weak* (i.e., for $^{14}\text{C} + ^{14}\text{C}$ and $^{16}\text{O} + ^{16}\text{O}$) or by (ii) irregular *intermediate structure*, some hundred kiloelectronvolts broad, if *inelastic coupling is strong* (i.e., for $^{12}\text{C} + ^{12}\text{C}$, $^{12}\text{C} + ^{16}\text{O}$, etc.). For less surface-transparent reactions, such as $^{18}\text{O} + ^{18}\text{O}$ (Ref. 7), etc., neither type of structure shows up in elastic scattering.

We would like to thank Dr. G. Korschinek for his help with the ^{14}C beam and Dr. H. J. Maier for providing us with a ^{14}C target. The help of Dr. W. Dahme during part of the data taking is acknowledged. This work was supported by the Bundesministerium für Forschung und Technologie. One of us (R. S.) is an Alexander von Humboldt Fellow.

^(a)Present address: North Eastern Hill University, Shillong, Indiana.

^(b)Permanent address: Jagellonian University, Cracow, Poland.

¹J. V. Maher, M. W. Sachs, R. H. Siemssen, A. Weidinger, and D. A. Bromley, *Phys. Rev.* **188**, 1665 (1969).

²R. Maier *et al.*, *Nucl. Instrum. Methods* **155**, 55 (1978).

³H. J. Maier, in Proceedings of the World Conference of the International Nuclear Target Developing Society, Boston, 1979 (to be published).

⁴J. G. Cramer *et al.*, *Nucl. Instrum. Methods* **111**, 425 (1973).

⁵R. A. Chatwin, J. S. Eck, D. Robson, and A. Richter, *Phys. Rev. C* **1**, 795 (1970).

⁶R. W. Shaw, Jr., R. Vandenbosch, and M. K. Mehta, *Phys. Rev. Lett.* **25**, 457 (1970).

⁷The $^5\text{He} + ^{23}\text{Ne}$ channel is open at $E_{c.m.} \leq 25$ MeV but is considered less important because of the rather large mass transfer involved.

⁸W. Trombik, thesis, Universität München, 1980 (unpublished).

⁹T. M. Cormier *et al.*, *Phys. Rev. Lett.* **38**, 940 (1977).

¹⁰Using the same set-up of two large NaI(Tl) detectors as for $^{14}\text{C} + ^{14}\text{C}$ we have also measured the mutual inelastic excitation for $^{16}\text{O} + ^{16}\text{O}$; the cross section rises from ~ 4 to ~ 16 mb at energies between 25 and 37 MeV (c.m.).

¹¹C. M. Jachcinski *et al.*, *Phys. Rev. C* **17**, 1263 (1978).

¹²The results obtained here support the double resonance model by H.-J. Fink, W. Scheid, and W. Greiner, *Nucl. Phys. A* **188**, 259 (1972).

¹³K. G. Bernhardt *et al.*, in *Nuclear Molecular Phenomena*, edited by N. Cindro (North-Holland, Amsterdam, 1978), p. 367.

Modified Heliocentric Coordinates for Particle Dynamics

Felix T. Smith

Molecular Physics Laboratory, SRI International, Menlo Park, California 94025

(Received 6 August 1980)

A modified heliocentric coordinate system is found for the dynamics of $n + 1$ particles that is barycentric, diagonalizes the kinetic energy, and is symmetric in n of the particles. The n planetary vectors are based on Radau's canonical point between the center of mass and the heliocenter. These coordinates, described by Radau in 1868 and forgotten, are especially valuable for describing centrosymmetric molecular fragments AB_n , and useful also for the mass polarization in atoms.

PACS numbers: 31.15.+q, 03.20.+i, 03.65.Fd, 33.10.Cs

Since the early days of planetary theory the heliocentric coordinate system has been a favorite for treating the motion of $n + 1$ particles, especially where one of them is dominant in mass or as a center of force.¹ It has the advantages that all the remaining n particles are treated in a formally symmetric way and that the number of degrees of freedom is reduced from $3(n + 1)$ to $3n$ by elimination of the motion of center of mass;

it has the disadvantage of cross terms in such expressions as the kinetic energy, moment of inertia and total orbital angular momentum. Jacobi² in 1842, in the three-body problem, introduced algebraically a set of coordinates that separates the center-of-mass motion while preserving the simple form of the major dynamical functions, by a procedure that in effect generates a chain of barycentric transformations applied successively